Distance Protection for Microgrids in Distribution System

Lin, Hengwei; Liu, Chengxi; Guerrero, Josep M.; Quintero, Juan Carlos Vasquez

Published in:
Proceedings of the 41th Annual Conference of IEEE Industrial Electronics Society, IECON 2015

DOI (link to publication from Publisher):
10.1109/IECON.2015.7392186

Publication date:
2015

Document Version
Accepted author manuscript, peer reviewed version

Distance Protection for Microgrids in Distribution System

Hengwei Lin[1] Chengxi Liu[2]
hwe@et.aau.dk chx@energinet.dk
1: Energy Technology Department
Aalborg University, 9220 Aalborg East, Denmark

Josep M. Guerrero[1] Juan C. Vásquez[1]
joz@et.aau.dk juq@et.aau.dk
2: Energinet.dk
Tonne Kjærsvej 65, Fredericia, DK-7000, Denmark

***Abstract*—Owing to the increasing penetration of distributed generation, there are some challenges for the conventional protection in distribution system. Bidirectional power flow and variable fault current because of the various operation modes may lead to the selectivity and sensitivity of the overcurrent protection decreased. This paper adopts distance protection for one mid-voltage level microgrid in Aalborg, Denmark. Different operation modes of the network are analyzed and tested in the paper. The simulation results show that the variations of the fault currents seen by the forward relays are much larger than the backward relays. Meanwhile, the fault currents change little with the randomness of renewable energy except the intermittence. Finally, it shows that the designed distance protection has satisfactory performance to clear the various faults.**

***Index Terms*—Distance Protection, Distributed Generation, Distribution System, Renewable Energy, Microgrid.**

I. INTRODUCTION

The drastic requirement to protect the environment from the climate led to the increase of the renewable generation. For the dispersed and uncertain characteristics of the nature source, most of the renewable generation units are installed on the transmission and distribution systems as micro-sources with the power electronic interfaces. However, the increasing penetration of the distributed generation (DG) brings challenges to the power system. In Denmark，more than 40% of the installed power generation has been from the renewable energy (RE), while most of the DGs are connected at the Distribution level (under 100 kV). On the electricity side, the focal points for the planning work still are ensuring sufficient generation capacity, managing system operation, and integrating large amounts of wind power and local electricity generation. The electricity infrastructure must support the increased use of renewable energy, and this places new demands on the system. As the basic infrastructure, the existing protection of the distribution system requires to be enhanced.

As an effective way, microgrids play more flexible roles to integrate these DGs in distribution girds than in the past. Majority of the distribution system and microgrids are operated in a radial way, though there are some loop feeders. Normally, these loops are opened with the relevant switches disconnected. It is only closed when there is a fault on the feeder. Therefore, the protection is designed for a radial way. Whereas, the existence of the renewable energy in the network will bring bidirectional power flow which makes the traditional overcurrent protection lose selectivity. Another difficulty is the low fault current in the islanded mode. The fault currents seen by the relays in the islanded mode become much lower than in the grid-connected mode. On the other hand, the renewable energy in the network often generates fluctuant power for its randomness feature. The settings for overcurrent relays are always designed under the assumption of the maximum operation mode to avoid the maximum start-up current. This start-up current can also appear after the fault has been cleared for the restoration of the generators, which is larger than the normal current. For the randomness, however, the fault current may become smaller in the minimum operation mode than in the maximum operation mode. In this situation, the different fault current levels may make the relay protection lose selectivity. Hence, the difference between the various operational modes calls for an update of the existing overcurrent relaying.

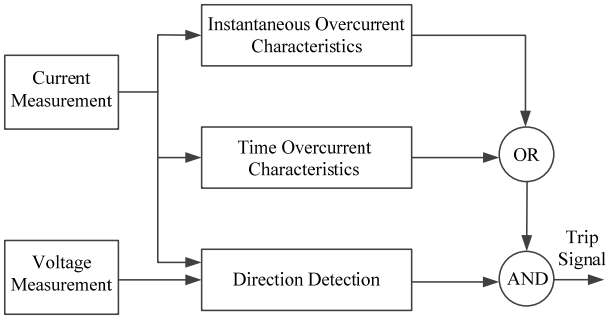

Fig. 1. The block diagram of directional overcurrent relay.

One of the normal solutions is to adopt directional overcurrent protection to replace the previous overcurrent protection. Some papers propose adaptive overcurrent protection which can modify the settings of the relays under different conditions [2-5]. The basic component of these protection strategies is the directional overcurrent relay that contains current transformer (CT) and voltage transformer (VT) to measure the current and the voltage respectively. The block diagram of the directional overcurrent relay is shown in Fig.1. The VT only contributes to the direction detection, while the measuring current participates both in the

overcurrent judgment and direction detection. The directional overcurrent relay has good direction selectivity. However, the sensitivity may be not satisfactory because the settings of the relays are still designed under the maximum operation mode assumption. The selectivity may also be decreased for this reason. In some situations, if the relay can not trip the fault in time, the renewable energy will be lost for its own protection tripping [6]. This problem can be solved by adaptive overcurrent protection with communication, but it requires significant investment in communication infrastructure. Moreover, the reliability may be affected by the complex configuration and setting groups.

Distance protection and differential protection are usually adopted in the transmission system which requires stricter selectivity and sensitivity than the distribution grids. Distance protection normally does not need communication between each relay [7-9]. Its main objection is to calculate the impedance at the fundamental frequency between the fault point and the relay location. The impedance is calculated from the measuring voltage and current at the relay point. According to the calculated impedance, the fault is identified whether within the protection zone. The characteristics will be expounded in Section III. Differential protection is another common method used to protect the transmission lines and transformers in power system [10-13]. Normally, it has the best selectivity since it depends on the communication between the beginning and the end of the protected line segment.

In this paper, the protection issues in power system with increasing RE are explained in Section I. A radial microgrid network in Aalborg, Denmark is given in Section II. The proposed distance relaying methodology, characteristic and relay design for the test system are presented in Section III. Section IV gives the study cases under different operation modes of the system to test the performance of distance protection. Finally, the conclusion is presented in Section V.

II. MODEL OF THE TEST DISTRIBUTION SYSTEM

The microgrid network is shown in Fig.2. It is a part of the distribution system owned by Himmerlands Elforsyning (HEF) in Aalborg, Denmark. This system contains a combined heat and power (CHP) plant with three 3.3MW gas turbine generators (GTGs) and three 630KW Wind Turbine Generators (WTGs). To consider the increasing renewable energy influence in the future local distribution network, these three small WTGs are modified to three small wind farms. Each wind farm consists of two 2WM doubly fed induction generators (DFIGs) and one 0.8MW capacitor bank. The configuration of Wind Farm 1 connected to Bus3 is shown in Fig.3. The minimum and maximum short circuit powers of the transmission grid are 224 MVA and 249 MVA, respectively.

The relays are denoted by "R" in Fig.1, while the numbers behind R represent the beginning bus and end bus in the primary protection zone. The microgrid has the ability to support all the loads during the islanded mode. Usually, it connects to the transmission grid represented by GRID, operating in the grid-connected mode. The connection of the wind farm is governed by the relays located at point of common coupling (PCC). PCC is the point in the public electricity supply network where the consumers are or can be connected. It is determined by the electricity supply undertaking. In this test system, these relays are all controlled by HEF, such as R31, R41 and R61. However, the interior of each wind farm is managed by its property owner respectively.

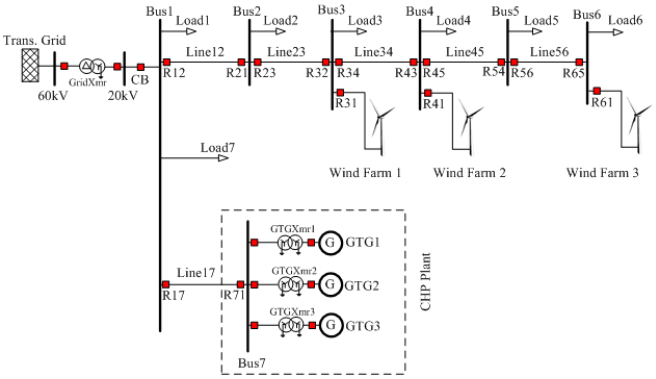

Fig. 2. The test distribution system.

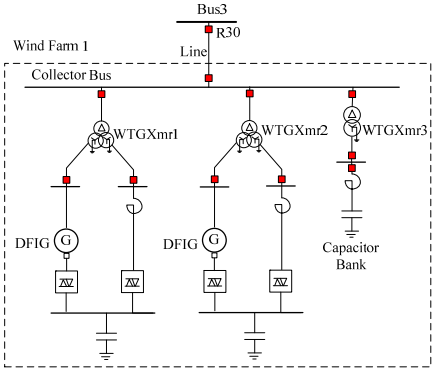

Fig. 3. Wind Farm 1.

III. DISTANCE PROTECTION

A. *Characteristic of Distance protection*

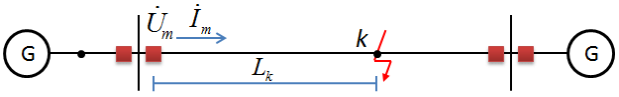

Fig. 4. The schematic diagram of distance protection.

The measuring impedance Z_m is calculated from the measuring voltage and current at the relay point, which is shown in equation (1). According to the calculated impedance, the fault is identified whether within the protection zone.

$$Z_m = \frac{\dot{U}_m}{\dot{I}_m} \tag{1}$$

When the system is under normal operation, Z_m is the load impedance Z_L. Whereas, Z_m will almost equal to the line impedance which is much smaller than Z_L if there is a fault in the line segment. Through calculating the measuring impedance and comparing it with the setting Z_{set} it realizes the detection and isolation of the fault.

Fig. 5 shows the simple schematic diagram of the distance relay. This figure does not show the signal processing part, starting component and power swing blocking element which exist in the industrial distance relay. The currents and voltages measured by CTs and VTs are sent to Zone 1, Zone 2 and Zone 3 respectively. Direction measurement in the relay is based on cross polarization to ensure dependable fault detection. As shown in Fig.5, there are 3 protection zones for forward faults. Z_{set}^{I} is applied to Zone 1 protection. Z_{set}^{II} is applied to Zone 2 which provides protection for the rest of the protected line not covered by Zone 1 and backup protection for the remote end bus. Z_{set}^{III} is applied to Zone 3 which provides remote back-up protection for the adjacent lines. It can be expressed as $Z_{set}^{\mathrm{I}} < Z_{set}^{\mathrm{II}} < Z_{set}^{\mathrm{III}}$. Zone 1 is an instantaneous protection, while Zone 2 and Zone 3 have definite time-stepped delay. In the paper, we define $T_D^{\mathrm{II}} = 0.35\mathrm{s}$ and $T_D^{\mathrm{III}} = 0.7s$.

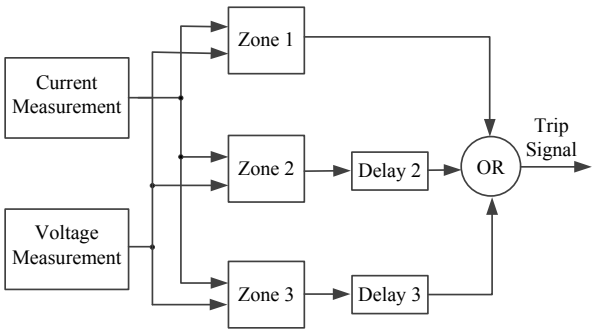

Fig. 5. The simple block diagram of time-stepped distance relay.

Distance protection with mho-based characteristics (forward direction) is adopted in this test. More characteristics can be extended if desired, such as offset mho element, reactance element, and blinder element etc. The selected characteristic here is a basic element in the industrial distance relay. Each protection zone of the relay has a circular characteristic which is shown in Fig.6. Through the amplitude comparison between Z_m and Z_{set}, the relay decides whether trip the breaker or not. If Z_m<Z_{set}, it means the fault occurs in the protection zone. On the contrary, the fault is not in the protection zone when Z_m>Z_{set}.

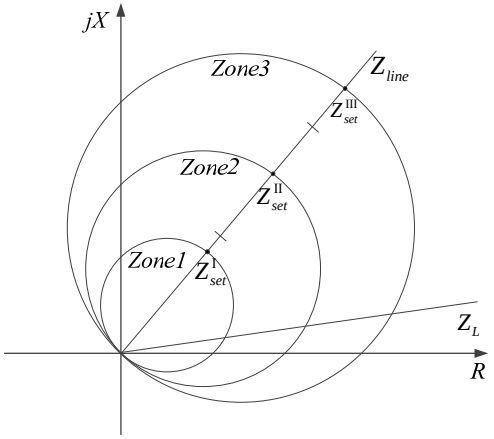

Fig. 6. Mho-based characteristics of distance relay.

B. *Design Settings of the Distance Relay*

As a rule of thumb, the setting impedances of each relay can be calculated through the below equations:

$$Z_{set}^{\mathrm{I}} = K_{rel}^{\mathrm{I}} Z_{line} \tag{2}$$

$$Z_{set}^{\mathrm{II}} = K_{rel}^{\mathrm{II}} (Z_{line} + Z_{set2}^{\mathrm{I}}) \tag{3}$$

$$Z_{set}^{\mathrm{III}} = K_{rel}^{\mathrm{III}} (Z_{line} + Z_{set2}^{\mathrm{II}}) \tag{4}$$

The suzper script in the equations represents the protection zone. K_{rel}^{I}, K_{rel}^{II}, K_{rel}^{III}, is the reliability coefficient of each protection zone, which is often set between 0.8 and 0.85. Z_{line} is the impedance of the primary protected line. Z_{set2}^{I} and Z_{set2}^{II} are the setting impedance of Zone 1 and Zone 2 for the downstream relay respectively.

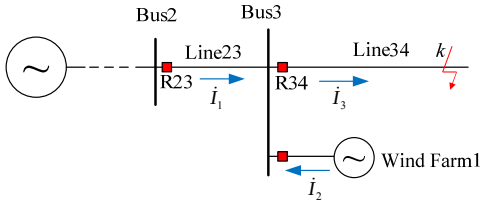

Fig. 7. Infeed current influence on the measuring impedance seen by R23.

In fact, the dispersed renewable generation brings infeed current for the settings of the relays. As shown in Fig. 7, Wind Farm 1 will feed the fault current if the fault occurs on Line34. The measuring impedance seen by R23 becomes larger than the impedance from Bus2 to the fault point (Z_{line23}+Z_k) for the infeed current of Wind Farm 1. The calculated impedance is given in equation (5):

$$Z_m = \frac{\dot{U}_m}{\dot{I}_m} = \frac{\dot{I}_1 Z_{line23} + \dot{I}_3 Z_k}{\dot{I}_1} \tag{5}$$

This measuring impedance seen by the upstream/downstream relay will be influenced seriously when the capacity of the dispersed renewable generation is non-ignorable and variable. In this situation, the measuring impedance becomes larger than the setting based on (3) when there is a fault on the downstream line segment. Furthermore, it leads to the selectivity decreased.

To offset the infeed current effect, the branch coefficient K_b is adopted for the setting impedance of the relay. From equation (5), taking R23 as an example, we can have:

$$K_b = \frac{\dot{I}_3}{\dot{I}_1} = \frac{\dot{I}_1 + \dot{I}_2}{\dot{I}_1} \tag{6}$$

Therefore, the equations for the settings of each relay should be rewritten with K_b below:

$$Z_{set}^{\mathrm{I}} = K_{rel}^{\mathrm{I}} Z_{line} \tag{7}$$

$$Z_{set}^{\mathrm{II}} = K_{rel}^{\mathrm{II}} (Z_{line} + K_b Z_{set2}^{\mathrm{I}}) \tag{8}$$

$$Z_{set}^{\mathrm{III}} = K_{rel}^{\mathrm{III}} (Z_{line} + K_b Z_{set2}^{\mathrm{II}}) \tag{9}$$

Through the calculation and test, the final time-distance diagram of protection settings is given in Fig.8.

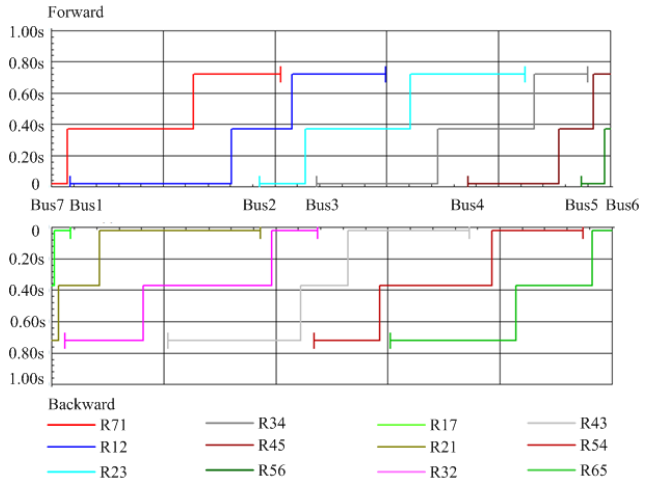

Fig. 8. The time-distance diagram of protection settings.

IV. CASE STUDY

For the network faults, it is not advisable to disconnect the wind farm immediately since the disconnection brings additional stress on the system. Therefore, the wind farm will not be disconnected as long as the frequency and voltage are not beyond the limits defined by the utility. According to the Danish grid code rendered in 2010, Fig.9 gives the requirements for tolerance of voltage drops for wind power plants with an output power greater than 1.5MW. The following requirements must be complied with for symmetrical and asymmetrical faults:

- Area A: The wind plant must keep connected to the network and sustain the normal production.
- Area B: The wind power plant must stay connected to the network. At the same time, the wind power plant must provide maximum voltage support by supplying a controlled amount of reactive power so as to ensure that the wind power plant helps uphold the voltage within the designed framework.
- Area C: Disconnecting the wind power plant is allowed.

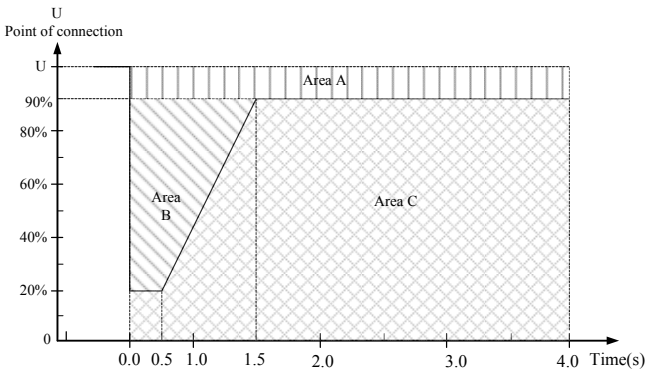

Fig. 9. Danish grid code demands for low voltage ride through.

R31, R41 and R61 at each PCC use inverse-time directional overcurrent relay (DOCR) since they are only responsible for each wind farm. The instantaneous pickup current I_{ins} is set 1.5 times of the rated current of the wind farm. For higher fault current (I>>), the relay pickup time is set fixed at t_{ins}. In this paper, t_{ins} is set at 50 ms. For lower fault current (I>), the relay pickup time is based on inverse time overcurrent characteristic. Following the standard inverse curve IEC60255-3, the characteristic is given below:

$$t = \frac{0.14T_p}{\left(\frac{I}{I_p}\right)^{0.02} - 1}(sec) \tag{10}$$

Where, T_p, I, I_p are time dial setting, fault current and pickup current. Finally, the time overcurrent plot of R31, R41 and R61 is shown in Fig. 10.

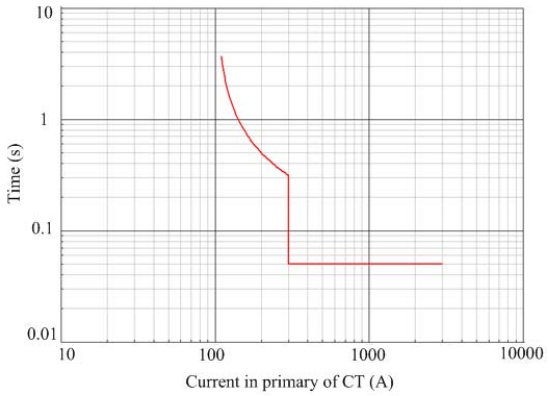

Fig. 10. Time overcurrent plot of R31, R41 and R61.

In the test, the pickup time of the distance relay is 20ms while the fault clearing time of the breaker is 60ms. All the WTGs in the wind farms contain the low voltage ride through (LVRT) scheme as shown in Fig.9. To analyze the variations of fault currents, four cases are considered with the same relay settings in DIgSILENT PowerFactory while a fault occurs at t=0 s.

- Case 1: The microgrid network is connected to the transmission line and all the wind farms operate in rated capacity.
- Case 2: The microgrid network is connected to the transmission line and all the wind farms operate in 20% rated capacity.
- Case 3: The microgrid network is operated in islanded mode and all the wind farms operate in rated capacity.
- Case 4: The microgrid network is operated in islanded mode and all the wind farms operate in 20% rated capacity.

A three phase fault, with fault resistance of 0.2Ω, is simulated at the middle of Line45. The states of circuit breakers (CBs) for all the four cases are given in Fig.11, while 1 means the state of CB is closed and 0 is open. Though the distribution system is operated in different modes, the trip time of the distance relay keeps the same. The reason is the distance relay decides whether the fault is in the protection zone through calculating the measuring impedance instead of the fault current.

The fault currents in Line45 are shown in Fig.12. The fault current seen from forward relay (R45) is higher than from backward relay (R54) due to the existence of CHP plant. At the same time, the fault current in grid-connected mode is larger than in islanded. This is owing to the capacity of transmission grid is much greater than the microgrid network.

On the other hand, the fault current seen by each relay changes little under different operation mode. It means that the randomness of DGs does not play significant role for the fault current. However, the intermittency still affects the selectivity of relays, since the relays may completely lose the support from DGs. From Fig.11, we can find that R54 trips slower than R45, since there is only Wind Farm 3 supporting the backward relays on Lin45 and Line56. Some additional protection strategies can be taken into account to enhance the performance of the backward relays for these two individual line segments. Whereas, the WTG in each wind farm keeps connected to the network for the fast fault clear in the test.

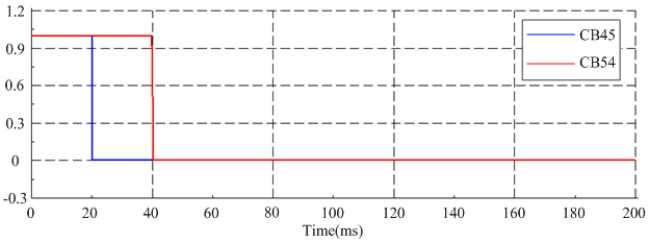

Fig. 11. States of CBs on Line45 for all the four cases.

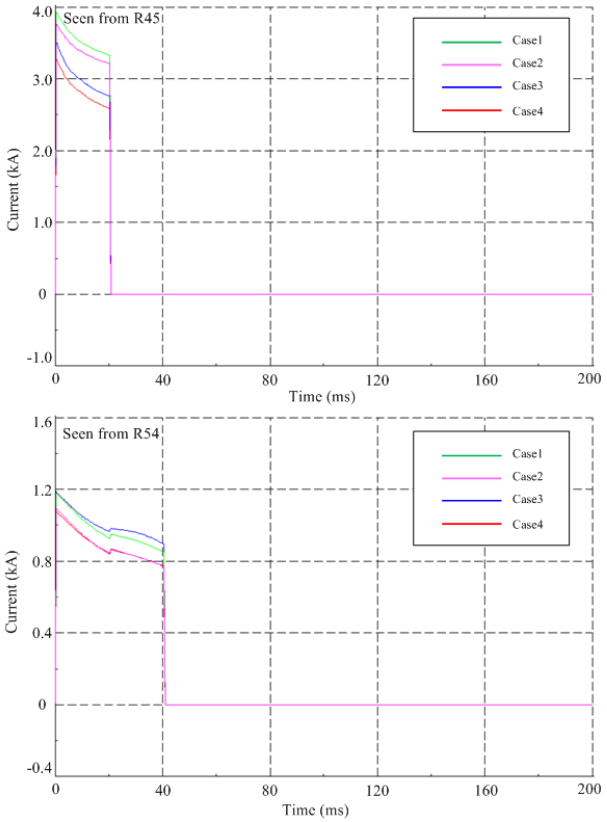

Fig. 12. Fault current in Line45 for all the four cases.

Another three phase fault with 0.3Ω fault resistance is simulated at the middle of Line12. The fault currents in Line12 are shown in Fig.14. Although the fault currents are prominently different for various operation modes, the tripping time remains fast and constant at 20ms.

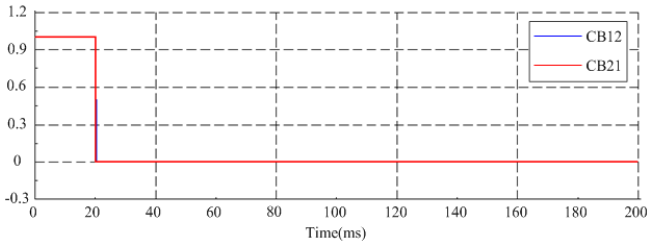

Fig. 13. States of CBs on Line12 for all the four cases.

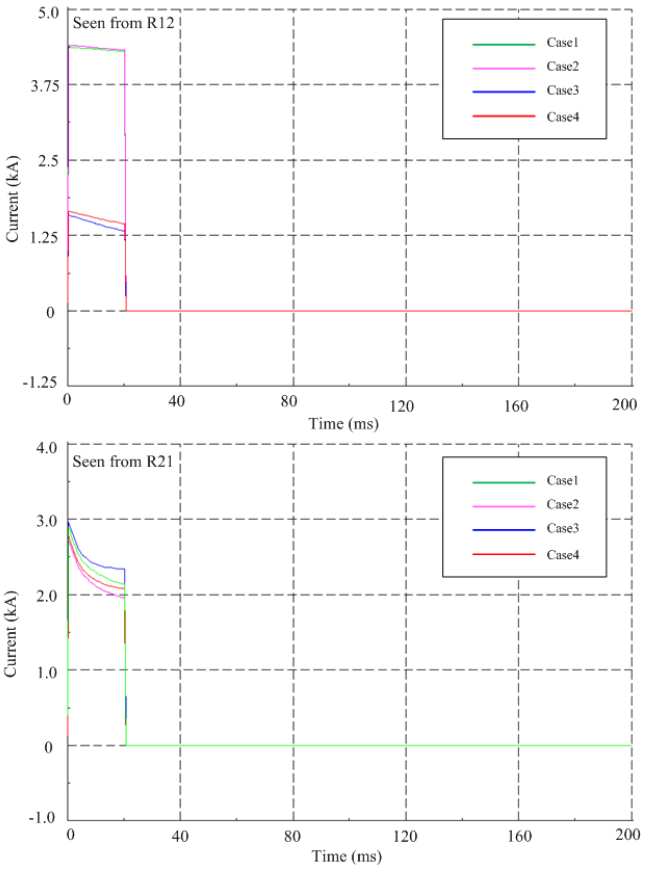

Fig. 14. Fault current in Line12 for all the four cases seen from Bus3.

The states of CBs for all the four cases are given in Fig.14. It shows that the fault current seen by the forward relay (R12) has much larger variation than the backward relay (R21). It is mainly due to the transmission system supporting the fault current considerably. The tripping time of distance relays have good selectivity and sensitivity when the system is operated in various modes, though the test here is in an ideal situation. For the real application of distance protection, it is a combination of multiple characteristics to handle the different faults in the system.

To test the relays which are responsible for protecting the wind farms, a three phase fault with fault resistance 5Ω in Wind Farm 3 is simulated. R61 trips at 50.3ms and clears the fault, which is shown in Fig.16. Since the utility here is not responsible for the intra of the wind farm, the protection strategy within the Wind Farm 3 is not discussed further in this paper.

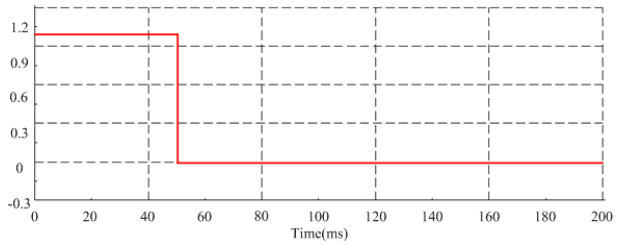

Fig. 15. Actual state of CB61.

V. CONCLUSION

Increasing DG penetration in the distribution system makes it possible to operate in the islanded mode as a microgrid. However, the existence of the renewable energy in the network brings bidirectional power flow. The fault current in the islanded mode is lower than in the grid-connected mode. The conventional overcurrent protection faces significant pressure for large integration of DGs, especially for the forward relays. Compared with overcurrent protection, the characteristic of distance protection changes little for different operation modes. The coordination between distance relay and other relays works well in the microgrid network. This paper also reveals the influence of RE on the distribution system. The intermittence of RE may affect the performance of the relays. On the other hand, the infeed current of RE affects the selectivity of the upstream relays. At the same time, a simple calculation method is adopted for distance relay settings considering the infeed current. Though only mho-based characteristic is tested in the paper, it reflects good selectivity and sensitivity under the different operation modes. Moreover，this paper reveals a complete protection design process for a microgrid. Further enhancement for the microgid protection will be considered in the near future.

Reference:

[1] G. D. Rockefeller, C. L. Wagner, J. R. Linders, K. L. Hicks, and D. T. Rizy, "Adaptive transmission relaying concepts for improved performance," *IEEE Trans. Power Delivery,* vol. 3, pp. 1446-1458, 1988.

[2] W. Hui, K. K. Li, and K. P. Wong, "An multi-agent approach to protection relay coordination with distributed generators in industrial power distribution system," in *Industry Applications Conference, 2005. Fourtieth IAS Annual Meeting. Conference Record of the 2005*, vol. 2, pp. 830-836 , 2005.

[3] W. Mu and C. Zhe, "Distribution system protection with communication technologies," in *IECON 2010 - 36th Annual Conference on IEEE Industrial Electronics Society*, pp. 3328-3333, 2010.

[4] Z. Q. Bo, "Adaptive non-communication protection for power lines BO scheme 1-The delayed operation approach," *IEEE Trans. Power Delivery,* vol. 17, pp. 85-91, 2002.

[5] Z. Q. Bo, "Adaptive non-communication protection for power lines BO scheme. II. The instant operation approach," *IEEE Trans. Power Delivery,* vol. 17, pp. 92-96, 2002.

[6] P. Mahat, C. Zhe, B. Bak-Jensen, and C. L. Bak, "A Simple Adaptive Overcurrent Protection of Distribution Systems With Distributed Generation," *IEEE Trans. Smart Grid,* vol. 2, pp. 428-437, 2011.

[7] J. Lorenc, A. Kwapisz, and K. Musierowicz, "Efficiency of admitance relays during faults with high fault resistance values in MV networks," *Power Tech, 2005 IEEE Russia*, pp. 1-5, 2005.

[8] A. H. Osman and O. P. Malik, "Transmission line distance protection based on wavelet transform," *IEEE Trans. Power Delivery,* vol. 19, pp. 515-523, 2004.

[9] Z. Zhang and D. Chen, "An Adaptive Approach in Digital Distance Protection," *IEEE J. Power Engineering Review,* vol. 11, p. 44, 1991.

[10] K. Yabe, "Power differential method for discrimination between fault and magnetizing inrush current in transformers," *IEEE Trans. Smart Grid,* vol. 12, pp. 1109-1118, 1997.

[11] W. D. Breingan, M. M. Chen, and T. F. Gallen, "The Laboratory Investigation of a Digital System for the Protection of Transmission Lines," *IEEE Trans. Power Apparatus and Systems,* vol. PAS-98, pp. 350-368, 1979.

[12] M. M. Eissa and O. P. Malik, "A new digital directional transverse differential current protection technique," *IEEE Trans. Power Delivery,* vol. 11, pp. 1285-1291, 1996.

[13] Y. Serizawa, M. Myoujin, K. Kitamura, N. Sugaya, M. Hori, A. Takeuchi, *et al.*, "Wide-area current differential backup protection employing broadband communications and time transfer systems," *IEEE Trans. Power Delivery,* vol. 13, pp. 1046-1052, 1998.